Thin Solid Films 589 (2015) 13–16

Contents lists available at ScienceDirect

Thin Solid Films

journal homepage: www.elsevier.com/locate/tsf

Controlled growth of $PbZr_{0.52}Ti_{0.48}O_3$ using nanosheet coated Si (001)

Anuj Chopra [a], Muharrem Bayraktar [b], Fred Bijkerk [c], Guus Rijnders [a,*]

[a] Inorganic Materials Science Group, MESA + Research Institute for Nanotechnology, University of Twente, PO Box 217, 7500 AE, The Netherlands
[b] Laser Physics and Nonlinear Optics Group, MESA + Research Institute for Nanotechnology, University of Twente, PO Box 217, 7500 AE, The Netherlands
[c] Industrial Focus Group XUV Optics, MESA + Research Institute for Nanotechnology, University of Twente, PO Box 217, 7500 AE, Enschede, The Netherlands

ARTICLE INFO

Article history:
Received 9 September 2014
Received in revised form 7 April 2015
Accepted 14 April 2015
Available online 22 April 2015

Keywords:
Piezoelectric properties
Nanosheets
Thin films
Silicon
Pulsed laser deposition
Lead zirconate titanate

ABSTRACT

Preferentially (001) and (110)-oriented $PbZr_{0.52}Ti_{0.48}O_3$ (PZT) films with a $LaNiO_3$ (LNO) bottom electrode were deposited on buffered Si (001) substrates using pulsed laser deposition. This high degree of control on growth orientation of these LNO and PZT thin films was achieved by using $Ca_2Nb_3O_{10}$ (CNO) and $Ti_{0.87}O_2$ nanosheets as buffer layers deposited on the Si by the Langmuir–Blodgett technique. The measured remnant polarization (P_r) and piezoelectric response of the (001)-oriented PZT films on CNO-nanosheets are 16 μC/cm^2 and 120 pm/V, respectively. These values are comparable to the values reported for the epitaxial PZT films grown on CeO_2/yttria-stabilized zirconia (YSZ) buffered Si substrates while the maximum deposition temperature is lowered from 800 °C to 600 °C which are the typical deposition temperatures of YSZ and PZT respectively. This lower maximum deposition temperature shows that the integration of PZT films by the nanosheet buffer layers is not limited to Si, but can be extended to substrates with low processing temperatures like glass for various device applications in the future.

1. Introduction

In recent years lead zirconate titanate, $Pb(Zr_xTi_{1-x})O_3$ (PZT), films have drawn much attention because of their potential use in microelectromechanical systems [1] and nonvolatile ferroelectric random access memories [2]. The properties of PZT films strongly depend on the composition (Zr/Ti ratio) therefore PZT (52/48) composition near the morphotropic phase boundary is commonly preferred due to its high piezoelectric response [3]. Moreover in order to utilize the optimal functional properties of PZT, high crystalline quality films with control on crystal-orientation is required [4]. Therefore, high quality epitaxial PZT films are usually prepared on single crystal oxide substrates such as $SrTiO_3$, MgO and $LaAlO_3$ using various physical and chemical vapor deposition techniques [5–8]. However, these substrates are expensive and therefore rarely used in practical applications. In the semiconductor industry, silicon (Si) substrates are commonly used, necessitating high quality growth of PZT on Si or Si-containing substrates. Integration of PZT on Si substrates and circuitry could pave the way to more efficient fabrication of devices. However, growth of oxide films, including PZT, directly on Si causes oxidation of the Si surface forming amorphous silicon oxide at the film–substrate interface, which is detrimental for growth of high quality crystalline films. As a result considerable efforts have been invested to find buffer layers that prevent such oxidation at the Si surface, allowing control of the crystal orientation of the subsequent layers. One way of growing oxides on Si is depositing yttria-stabilized zirconia (YSZ) and then CeO_2 as buffer layers [9–12]. There are also efforts to integrate preferentially oriented PZT on platinized Si substrates at lower temperatures, but issues like control of the growth orientation and fatigue are still to be overcome for a stable and reproducible response of PZT [13,14]. Ferroelectric and piezoelectric properties are highly anisotropic, thus integration of PZT on Si with control of the growth orientation is highly desired [4]. Orientation-control on growth direction is usually achieved by using $SrRuO_3$ or $LaNiO_3$ (LNO) electrodes on YSZ and/or CeO_2 buffer layers. However, growth of YSZ and CeO_2 on Si is usually achieved at very high temperatures (750–800 °C) [9–12] which would create problems for any circuitry on the same substrate. In addition, such a high temperature growth process is not very suitable for the integration of PZT on substrates like glass. The attempts on growing at lower temperatures have practically resulted in poor crystalline quality, i.e. secondary pyrochlore phase or polycrystalline, PZT films [15–17]. Hence in order to integrate PZT on cost effective substrates such as Si and glass, development of integration processes with lower processing temperature is required.

Recently two-dimensional materials such as oxide nanosheets have attracted attention due to their physical properties and potential use in a wide range of applications such as dielectrics and semiconductors [18–21]. The advantage of the nanosheets is that they can be transferred in crystalline form to the substrates such as Si and glass at room temperature. Contrary to the major attention from the dielectric and semiconductor applications, little attention has been paid on the potential use of the nanosheets as a buffer/seed layer to promote piezoelectric film growth [22,23]. On the other hand, these works [22,23] use chemical

* Corresponding author at: University of Twente, Inorganic Materials Science Group, Enschede, The Netherlands. Tel.: +31 53 4892618; fax: +31 53 4892990.
E-mail address: a.j.h.m.rijnders@utwente.nl (G. Rijnders).

http://dx.doi.org/10.1016/j.tsf.2015.04.039
0040-6090/

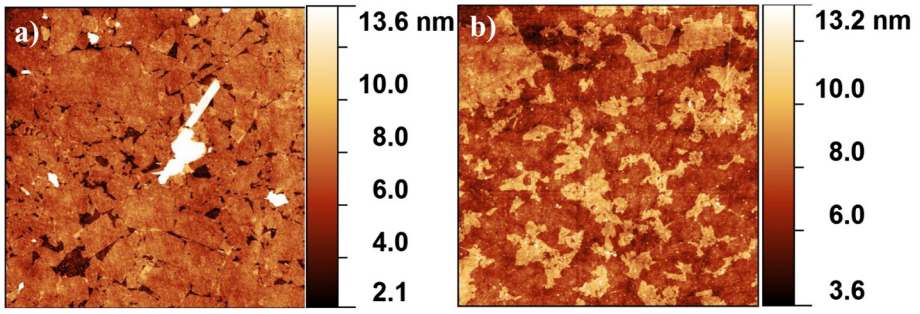

Fig. 1. AFM images recorded in 20 × 20 μm^2 area for (a) $Ca_2Nb_3O_{10}$ and (b) $Ti_{0.87}O_2$-nanosheets revealing high area coverage.

solution deposition for growth of Ti rich compositions of PZT and the produced films suffer from mixed growth and high coercive fields. In addition, no data is reported regarding the piezoelectric properties of the PZT films, which is indeed crucial for the device applications. There is no detailed investigation in the literature on control of growth direction of PZT (52/48) films using $Ca_2Nb_3O_{10}$ (CNO) and $Ti_{0.87}O_2$ (TO) nanosheets as buffer layers on Si substrates. In this article, we report the controlled growth of the (001) and (110)-oriented PZT/$LaNiO_3$ (LNO) films using CNO and TO nanosheets as buffer layers, respectively on Si substrates. Comparable ferroelectric and piezoelectric properties were measured for both (001) and (110)-oriented PZT films. We used pulsed laser deposition (PLD) which is known to give better control on the stoichiometry and crystal orientation. The entire growth process was achieved at temperatures lower than 600 °C, which allows the integration of PZT also on glass.

2. Experimental procedure

CNO and TO-nanosheet films were transferred from a single layer CNO and TO colloidal solution using the Langmuir–Blodgett (LB) technique at room temperature. The solutions of CNO and TO-nanosheets were prepared by exfoliation of layered $HCa_2Nb_3O_{10}\cdot 1.5\ H_2O$ and $H_{1.7}Ti_{1.73}O_4\cdot H_2O$ respectively, by using tetrabutylammonium hydroxide [21–24]. The nanosheet films with layer number of >3 are not stable at temperatures higher than 650 °C [25], thus only 1 layer of CNO and 2 layers of TO-nanosheets were deposited on Si substrates. Prior to the deposition of the PZT/LNO stack, the nanosheet buffered Si (001) substrates were annealed at 600 °C for 60 min in a 0.140 mbar oxygen atmosphere. This step was required to burn out the surfactant used to grow the nanosheets and increase the adhesion between substrate and nanosheets. Surface morphology of the nanosheets was investigated by a Bruker Dimension Icon atomic force microscope (AFM) using tapping mode. Fig. 1(a) and (b) shows 20 × 20 μm^2 AFM images of the CNO and TO-nanosheets. The AFM images show deposition of CNO and TO nanosheets on Si substrates with high area coverage.

All films were deposited in situ using PLD by ablating materials from stoichiometric targets of LNO and PZT with KrF excimer laser pulses at 248 nm wavelength with 20 ns pulse duration. A base pressure of 5×10^{-5} Pa was maintained in the deposition chamber before raising the substrate temperature. PZT films with 750 nm thickness were sandwiched between 200 nm thick bottom and 100 nm thick top LNO electrodes respectively. In order to avoid any degradation of PZT phase, the top LNO electrode layer was deposited at the same growth temperature as of PZT (585 °C). Later on, 100 nm thick Pt was sputtered on the LNO top electrode by radio frequency sputtering at room temperature to increase the homogeneity of the electric field. After the depositions, top electrode was patterned into capacitors with 200 × 200 μm^2 area using standard photolithography process and structured by argon etching.

Crystallographic characterization was performed by means of a Philips X'Pert MRD X-ray diffractometer (XRD) using Cu-*Kα* radiation. The scanning electron microscopy (SEM) images of both of the heterostructures were recorded using a Zeiss MERLIN HR-SEM. The polarization–electric field (*P*–*E*) hysteresis loop and the switching current–electric field (*I*–*E*) characteristics of the PZT films were recorded with a ferroelectric tester (TF analyzer 2000, aixACCT). The ferroelectric

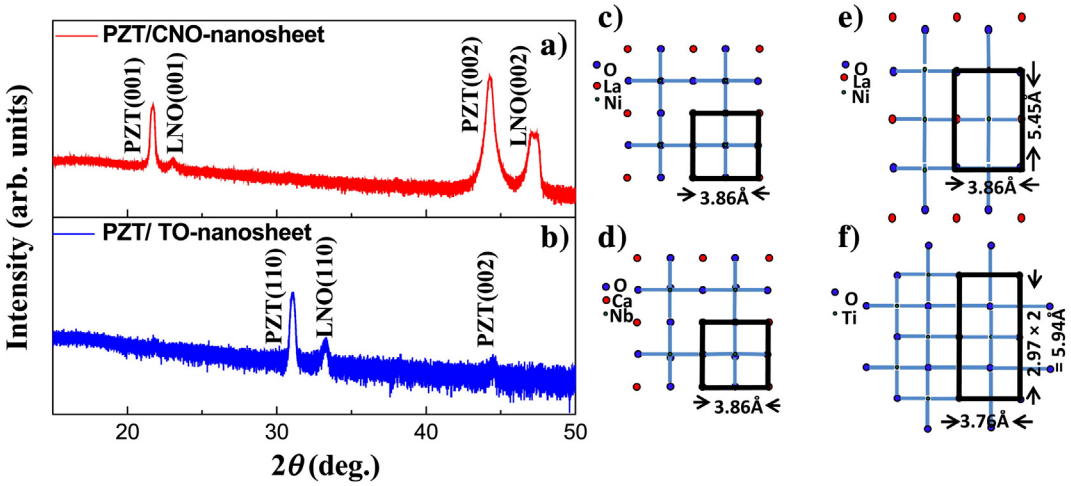

Fig. 2. XRD *θ*–2*θ* scan of PZT films revealing (a) (001) on $Ca_2Nb_3O_{10}$/Si. (b) (110)-orientation on $Ti_{0.87}O_2$/Si substrates. Since the nanosheets are only a few unit cells thick, they are not visible in the XRD measurements. A schematic demonstration of (c–d) the ideal fitting of the $LaNiO_3$ (100) plane lattice parameters to the $Ca_2Nb_3O_{10}$ lattice parameters, (e–f) the match of $LaNiO_3$ (110) plane lattice parameters and $Ti_{0.87}O_2$ lattice parameters.

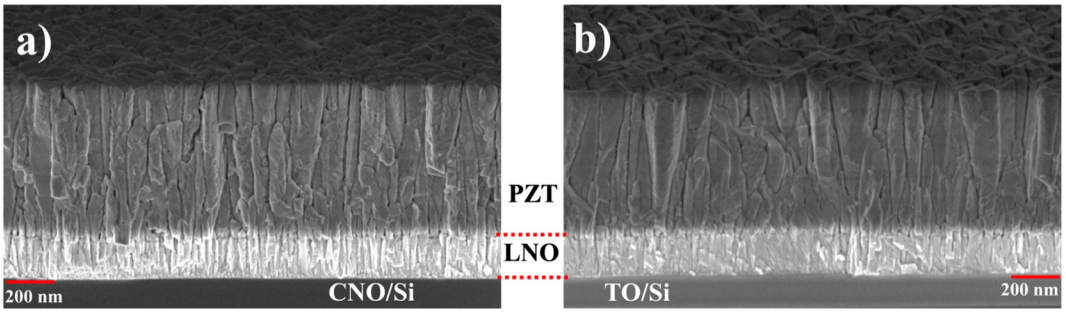

Fig. 3. SEM images of PZT films on (a) LNO/CNO/Si and (b) LNO/TO/Si.

hysteresis loops were measured using bipolar triangular pulses at 1 kHz. The piezoelectric response of the films was measured using a Polytec MSA-400 laser Doppler vibrometer (LDV) operating at 8 kHz.

3. Results and discussion

The XRD patterns of PZT and LNO films on CNO and TO-nanosheet buffered Si (001) substrates (pseudo-cubic indexing is used for all) are shown in Fig. 2(a) and (b). The PZT films consist of a pure perovskite phase and no pyrochlore phase was observed in both heterostructures. Fig. 2(a) and (b) shows that PZT films grown on CNO and TO-nanosheets have (001)-orientation and (110)-orientation, respectively. The CNO-nanosheet had a 2D square lattice with a lattice parameter of a = 3.86 Å, which is an exact fit to that of the (001) face of the cubic LNO (a = 3.86 Å). This exact fit of lattice parameters promotes (001)-growth of both LNO and PZT on CNO-nanosheets as schematically shown in Fig. 2(c–d) and observed in the XRD patterns. TO-nanosheets have a lepidocrocite-type structure with a 2D rectangular lattice with lattice parameter of a = 3.76 Å and b = 2.97 Å [20]. On TO nanosheets, besides having a lower lattice mismatch along a-parameter (2.5%), (001)-oriented growth of LNO was not possible due to large lattice mismatch along b-parameter (23%). On the other hand, the two-fold cell of a TO-nanosheet provides a close match to the (110) unit cell of LNO (~9%) as schematically shown in Fig. 2(e–f). This promotes (110)-oriented growth of both LNO and PZT. However, nanosheets are randomly oriented in-plane, thus the subsequent layers are also expected to be randomly oriented in-plane. The microstructure of the PZT films deposited on CNO and TO-nanosheet buffered Si substrate was further investigated by SEM as shown in Fig. 3(a) and (b), respectively. Cross-sectional SEM images reveal thicknesses around 600 nm and 200 nm for the PZT film and LNO electrode layer, respectively. It has been observed from the SEM images that PZT films show a columnar type of growth for both heterostructures due to the large lattice mismatch (~5%) between LNO and PZT.

The polarization–electric field (*P*–E) hysteresis and switching current–electric field (*I*–*E*) which were measured at 1 kHz for two heterostructures are shown in Fig. 4(a) and (b) respectively. Despite having different crystal-orientations for PZT films the remnant polarization (P_r) and coercive field (E_c) for both of the heterostructures are comparable. The remnant polarization (P_r), and coercive field (E_c) for both structures are 16 μC/cm^2 and 32 kV/cm respectively, which is comparable to the values reported for the epitaxial PZT films on buffered Si substrates [12]. Well saturated hysteresis loops and sharp switching peaks observed in ferroelectric measurements show that the quality of these PZT films on nanosheets is comparable to the quality of epitaxial PZT films reported on YSZ\$CeO_2$buffered Si substrates [12]. Furthermore, the piezoelectric response of the PZT film was locally measured using LDV. The samples were fixed to large metal plates with silver paste to prevent any contribution of the bending of the substrates to the LDV measurements. The piezoelectric hysteresis loops shown in Fig. 5 were measured at electrodes with 200 × 200 μm^2 area in response to a small AC electric field of ~6.7 kV/cm. This AC electric field was superimposed on a DC electric field sweeping from −170 kV/cm to +170 kV/cm. The maximum effective piezoelectric response ($d_{33,f}$) measured for PZT films on CNO and TO-nanosheets are 120 pm/V and 108 pm/V, respectively. These values are higher as compared to the values reported for the PZT films by LDV [26,27], which shows the high quality of PZT films on nanosheets buffered Si substrates.

In summary, a high degree of control on the crystal growth orientation of PZT films on Si substrates is achieved by incorporating CNO and TO-nanosheets. The results reveal that the PZT films deposited on such nanosheets have comparable ferroelectric properties, and superior piezoelectric properties were obtained as compared to the films deposited without the use of nanosheets. This paper shows that integration of PZT films at low temperature with control on crystal-orientation to the Si-based devices is possible, a process which is expected to have a positive impact on many practical applications of piezoelectric films.

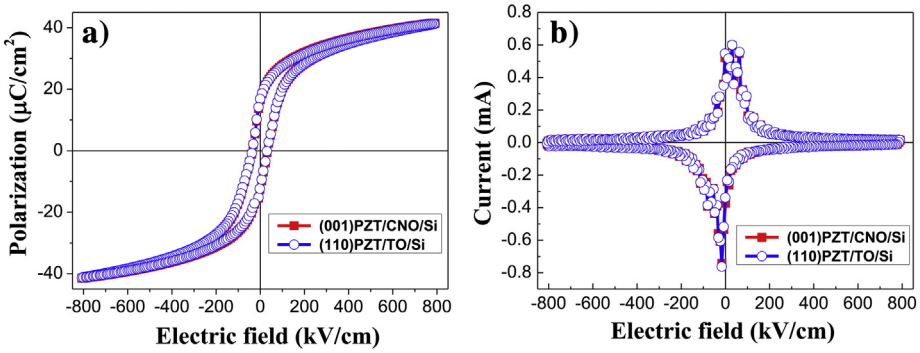

Fig. 4. (a) Macroscopic polarization–electric field hysteresis and (b) switching current–electric field curves of PZT films on $Ca_2Nb_3O_{10}$ and $Ti_{0.87}O_2$-nanosheets revealing that PZT films could be switched in either direction.

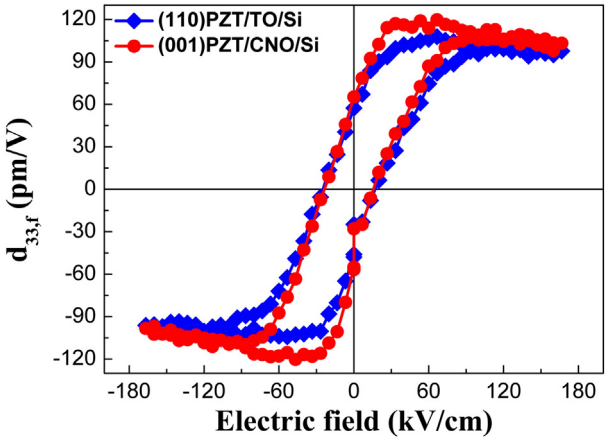

Fig. 5. The piezoelectric hysteresis ($d_{33,f}$) loops measured by LDV for PZT films on $Ca_2Nb_3O_{10}$ and $Ti_{0.87}O_2$-nanosheets.

Acknowledgment

This research program is funded by "Stichting Technologie en Wetenschap (STW)" under the contract 10448 with the project name "Smart Multilayer Interactive Optics for Lithography at Extreme UV wavelengths (SMILE)". The authors would like to thank Prof. J. E. ten Elshof and Mr. Maarten Nijland for providing the nanosheets and Dr. Minh Nguyen for Pt coating.

References

[1] S. Trolier-McKinstry, P. Muralt, Thin film piezoelectrics for MEMS, J. Electroceram. 12 (2004) 7.
[2] M. Okuyama, Y. Ishibashi (Eds.), Ferroelectric Thin Films: Basic Properties and Device Physics for Memory Applications, Springer-Verlag, Berlin Heidelberg, 2005.
[3] B. Jaffe, W.R. Cook Jr., H. Jaffe, Piezoelectric Ceramics, Academic Press Inc., London, 1971.
[4] X. Du, J. Zheng, U. Belegundu, K. Uchino, Crystal orientation dependence of piezoelectric properties of lead zirconate titanate near the morphotropic phase boundary, Appl. Phys. Lett. 72 (1998) 2421.
[5] L.X. Cao, Y. Xu, B.R. Zhao, L.P. Guo, L. Li, B. Xu, Y.Z. Zhang, H. Chen, A.J. Zhu, Z.H. Mai, J.H. Zhao, Y.F. Fu, X.J. Li, A structural investigation of high-quality epitaxial Pb(Zr, Ti)O_3 thin films, J. Phys. D 30 (1997) 1455.
[6] I. Vrejoiu, G. Le Rhun, L. Pintilie, D. Hesse, M. Alexe, U. Gösele, Intrinsic ferroelectric properties of strained tetragonal $PbZr_{0.2}Ti_{0.8}O_3$ obtained on layer-by-layer grown, defect-free single-crystalline films, Adv. Mater. 18 (2006) 1657.
[7] G. Barucca, A. De Benedittis, A. Di Cristoforo, G. Majni, P. Mengucci, F. Leccabue, B.E. Watts, Crystallisation of perovskite PZT films on MgO substrates, Thin Solid Films 319 (1998) 207.
[8] J.H. Kim, F.F. Lange, Seeded epitaxial growth of $PbTiO_3$ thin films on (001) $LaAlO_3$ using the chemical solution deposition method, J. Mater. Res. 14 (1999) 1626.
[9] D.K. Fork, D.B. Fenner, G.A.N. Connell, J.M. Phillips, T.H. Geballe, Epitaxial yttria-stabilized zirconia on hydrogen-terminated Si by pulsed laser deposition, Appl. Phys. Lett. 57 (1990) 1137.
[10] S.J. Wang, C.K. Ong, L.P. You, S.Y. Xu, Epitaxial growth of yittria-stabilized zirconia oxide thin film on natively oxidized silicon wafer without an amorphous layer, Semicond. Sci. Technol. 15 (2000) 836.
[11] A. Chopra, D. Pantel, Y. Kim, M. Alexe, D. Hesse, Microstructure and ferroelectric properties of epitaxial cation ordered $PbSc_{0.5}Ta_{0.5}O_3$ thin films grown on electroded and buffered Si(100), J. Appl. Phys. 114 (2013) 084107.
[12] M. Dekkers, M.D. Nguyen, R. Steenwelle, P.M. te Riele, D.H.A. Blank, G. Rijnders, Ferroelectric properties of epitaxial Pb(Zr, Ti)O_3 thin films on silicon by control of crystal orientation, Appl. Phys. Lett. 95 (2009) 012902.
[13] J.G.E. Gardeniers, A. Smith, C. Cobianu, Characterisation of sol–gel PZT films on Pt-coated substrates, J. Micromech. Microeng. 5 (1995) 153.
[14] A. Kumar, M.R. Alam, A. Mangiaracina, M. Shamsuzzoha, Synthesis of the PZT films deposited on Pt-coated (100) Si substrates for nonvolatile memory applications, J. Electron. Mater. 26 (1997) 1331.
[15] A. Rajashekhar, A. Fox, S.S.N. Bharadwaja, S. Trolier-McKinstry, In situ laser annealing during growth of $Pb(Zr_{0.52}Ti_{0.48})O_3$ thin films, Appl. Phys. Lett. 103 (2013) 032908.
[16] Masanori Aratani, Takahiro Oikawa, Tomohiko Ozeki, Hiroshi Funakubo, Epitaxial-grade polycrystalline Pb(Zr, Ti)O_3 film deposited at low temperature by pulsed-metalorganic chemical vapor deposition, Appl. Phys. Lett. 79 (2001) 1000.
[17] K.C. Chena, A. Janaha, J.D. Mackenziea, Crystallization of oxide films derived from metallo-organic precursors, MRS Proc. 72 (1986).
[18] M. Osada, K. Akatsuka, Y. Ebina, Y. Kotani, K. Ono, H. Funakubo, S. Ueda, K. Kobayashi, K. Takada, T. Sasaki, Langmuir–Blodgett fabrication of nanosheet-based dielectric films without an interfacial dead layer, Jpn. J. Appl. Phys. 47 (2008) 7556.
[19] R. Ma, T. Sasaki, Nanosheets of oxides and hydroxides: ultimate 2D charge-bearing functional crystallites, Adv. Mater. 22 (2010) 5082.
[20] T. Shibata, H. Takano, Y. Ebina, D.S. Kim, T.C. Ozawa, K. Akatsuka, T. Ohnishi, K. Takada, T. Kogure, T. Sasaki, Versatile van der Waals epitaxy-like growth of crystal films using two-dimensional nanosheets as a seed layer: orientation tuning of $SrTiO_3$ films along three important axes on glass substrates, J. Mater. Chem. C 2 (2014) 441.
[21] M. Nijland, S. Kumar, R. Lubbers, D.H.A. Blank, G. Rijnders, G. Koster, J.E. ten Elshof, Local control over nucleation of epitaxial thin films by seed layers of inorganic nanosheets, ACS Appl. Mater. Interfaces 6 (2014) 2777.
[22] K. Kikuta, K. Noda, S. Okumura, T. Yamaguchi, S. Hirano, Orientation control of perovskite thin films on glass substrates by the application of a seed layer prepared from oxide nanosheets, J. Sol-Gel Sci. Technol. 42 (2007) 381.
[23] Y. Minemura, K. Nagasaka, T. Kiguchi, T.J. Konno, H. Funakubo, H. Uchida, Fabrication and evaluation of one-axis oriented lead zirconate titanate films using metal-oxide nanosheet interface layer, Jpn. J. Appl. Phys. 52 (2013) 09KA04.
[24] A. Kumar, S.K.C. Palanisamy, J.M. Boter, C. Hellenthal, J.E. ten Elshof, H.J.W. Zandvliet, Imaging of $Ti_{0.87}O_2$ nanosheets using scanning tunneling spectroscopy, Appl. Surf. Sci. 265 (2013) 201.
[25] K. Fukuda, Y. Ebina, T. Shibata, T. Aizawa, I. Nakai, T. Sasaki, Unusual crystallization behaviors of anatase nanocrystallites from a molecularly thin titania nanosheet and its stacked forms: increase in nucleation temperature and oriented growth, J. Am. Chem. Soc. 129 (2007) 202.
[26] S. Sivaramakrishnan, P. Mardilovich, A. Mason, A. Roelofs, T. Schmitz-Kempen, S. Tiedke, Electrode size dependence of piezoelectric response of lead zirconate titanate thin films measured by double beam laser interferometry, Appl. Phys. Lett. 103 (2013) 132904.
[27] M. Bayraktar, A. Chopra, F. Bijkerk, G. Rijnders, Nanosheet controlled epitaxial growth of $PbZr_{0.52}$ $Ti_{0.48}$ O_3 thin films on glass substrates, Appl. Phys. Lett. 105 (2014) 132904.